

Imaging neuroinflammation with PET - an overview of studies from Manchester

Rainer Hinz

06 December 2019

Friday Imaging Meeting

Stopford G.706 / WMIC first floor meeting room

Introduction

Translocator Protein 18kDa (TSPO)

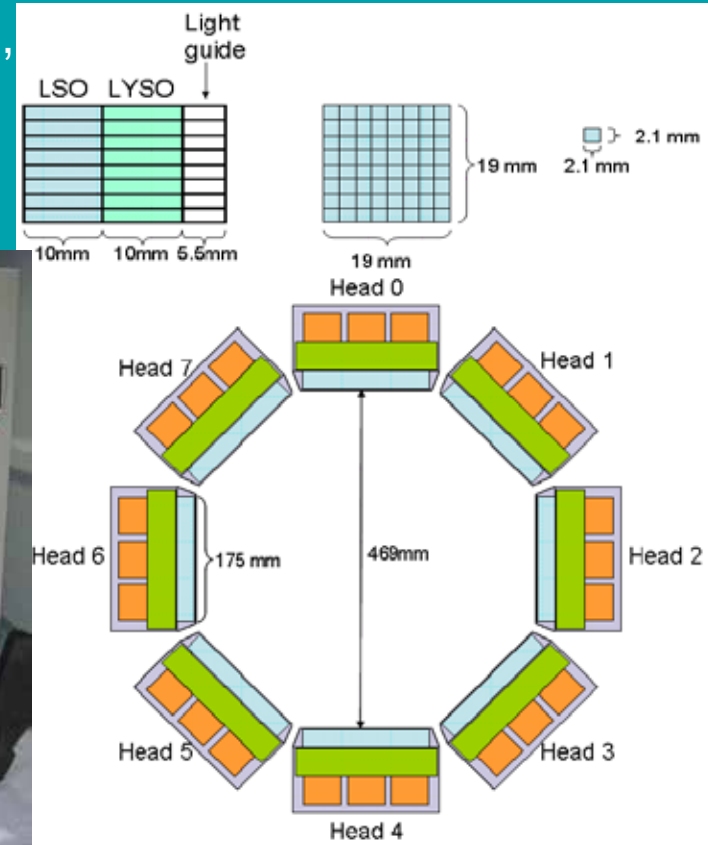
- is a nuclear encoded mitochondrial protein.
- is abundant in peripheral organs (particularly adrenal glands and kidney) and haematogenous cells.
- its function still needs full elucidation but it plays an important role in steroid synthesis and in the regulation of immunological responses in mononuclear phagocytes.

TSPO in diseases of the Central Nervous System (CNS)

- High levels have been observed in infiltrating blood-borne cells and activated microglia.
- Significant microglial activation occurs after mild to severe neuronal damage resulting from traumatic, inflammatory, degenerative and neoplastic disease.
- Microglia are activated in the surroundings of focal lesions but also in the distant, anterograde and retrograde projection areas of the lesioned neural pathway.

Methods

- High Resolution Research Tomograph (HRRT),
- dual layer LSO/LYSO scintillator crystals,
- intrinsic spatial resolution of about 2.5 mm.



Siemens Inveon small animal PET-CT

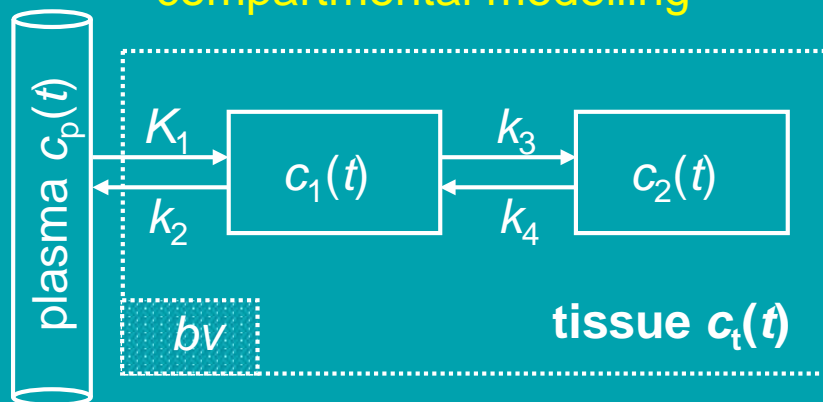
Positron Emission Tomography (PET) of TSPO in the Brain

Radiotracers used in clinical research

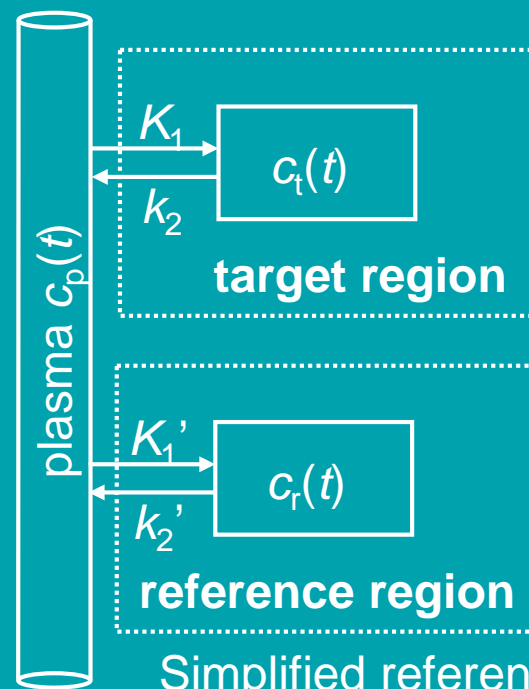
- From the 1980ies: [^{11}C]Ro 5-4864, racemic [^{11}C]PK11195.
- Since the early 1990ies: enantiomerically pure [^{11}C](*R*)-PK11195.
- For the last 15 years “second generation” tracers with higher affinity: [^{11}C]DPA-713, [^{18}F]DPA-714, [^{18}F]F-DPA, [^{123}I]CLINDE, [^{11}C]DAA1106, [^{18}F]PBR06, [^{11}C]PBR28, [^{18}F]PBR111, [^{18}F]FEPPA, [^{11}C]vinpocetine, [^{18}F]GE-180, [^{11}C]ER176, ...

Quantification approaches

Plasma input function
 compartmental modelling



Two-tissue compartment model (2TCM)



Simplified reference
 tissue model (SRTM)

Brain inflammation is induced by co-morbidities and risk factors for stroke

Caroline Drake^a, Hervé Boutin^a, Matthew S. Jones^b, Adam Denes^a, Barry W. McColl^{a,1}, Johann R. Selvarajah^c, Sharon Hulme^c, Rachel F. Georgiou^c, Rainer Hinz^b, Alexander Gerhard^b, Andy Vail^d, Christian Prenant^b, Peter Julyan^e, Renaud Maroy^f, Gavin Brown^b, Alison Smigova^b, Karl Herholz^b, Michael Kassiou^{g,h,i}, David Crossman^j, Sheila Francis^k, Spencer D. Proctor^l, James C. Russell^l, Stephen J. Hopkins^c, Pippa J. Tyrrell^c, Nancy J. Rothwell^a, Stuart M. Allan^{a,*}

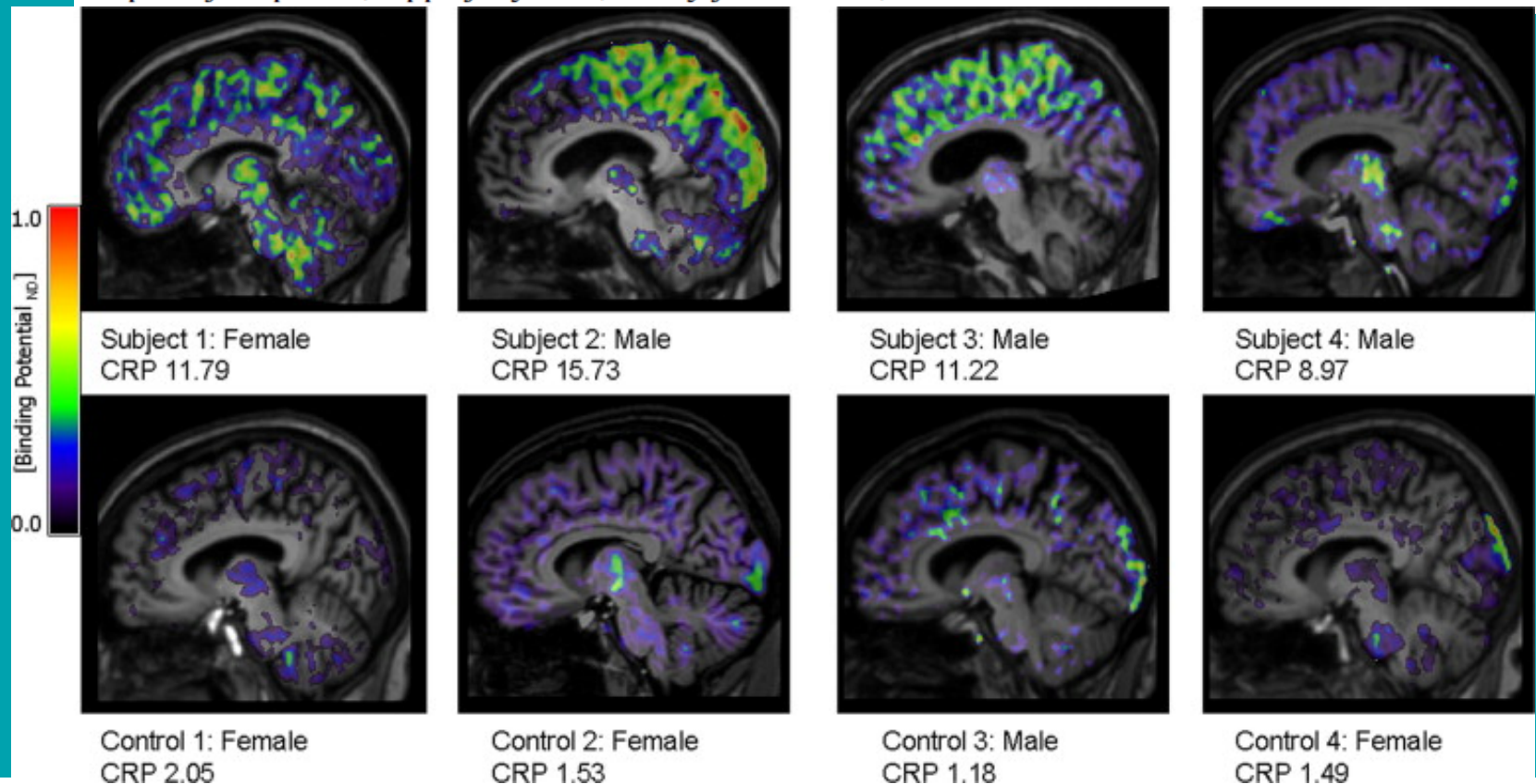


Fig. 6. [¹¹C](R)-PK11195 binding potential (BP_{ND}) images are shown for all subjects and control participants. Images are displayed on each subject's respective T1 MRI scan normalised to the SPM5 T1 brain template. The value for each individual's CRP at the time of PET scanning is also shown.

[¹⁸F]DPA-714: Direct Comparison with [¹¹C]PK11195 in a Model of Cerebral Ischemia in Rats

Hervé Boutin^{1,2*}, Christian Prenant², Renaud Maroy³, James Galea^{4,5}, Andrew D. Greenhalgh^{4a}, Alison Smigova², Christopher Cawthorne², Peter Julyan⁶, Shane M. Wilkinson⁷, Samuel D. Banister⁷, Gavin Brown², Karl Herholz², Michael Kassiou^{7,8,9}, Nancy J. Rothwell⁴

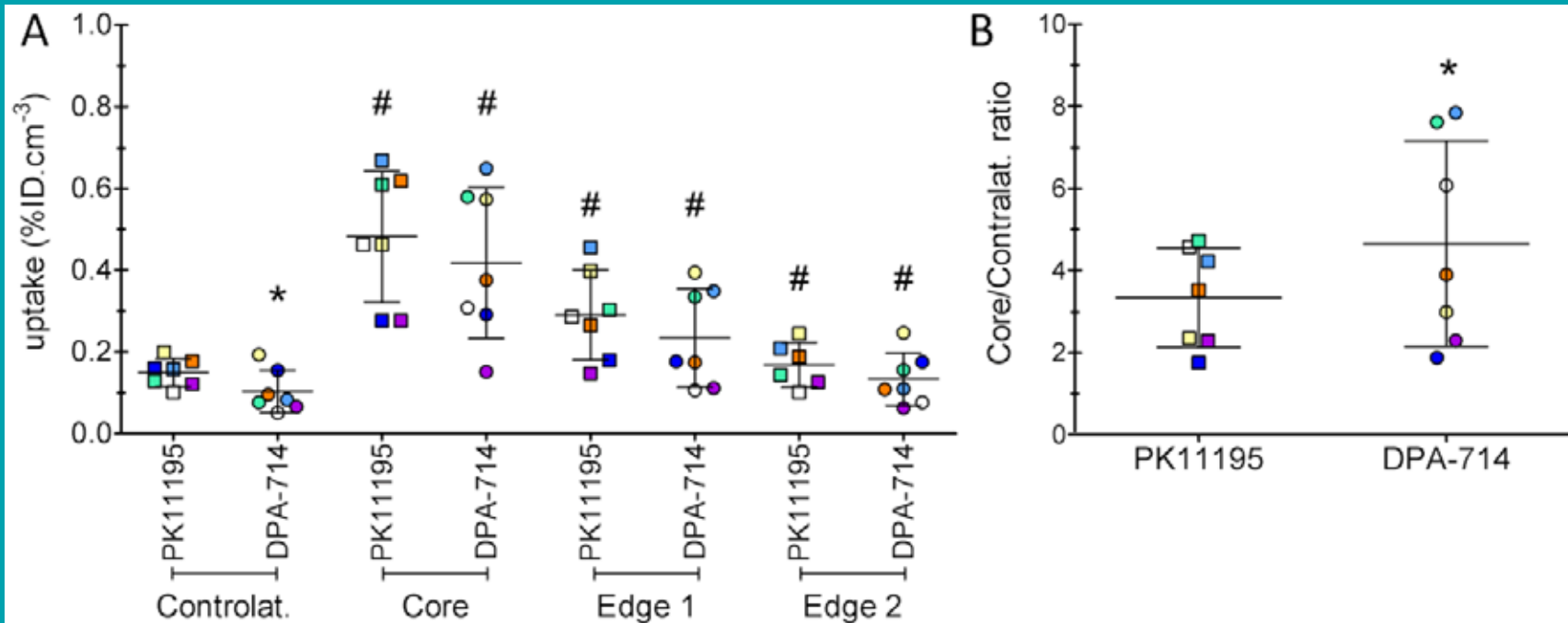
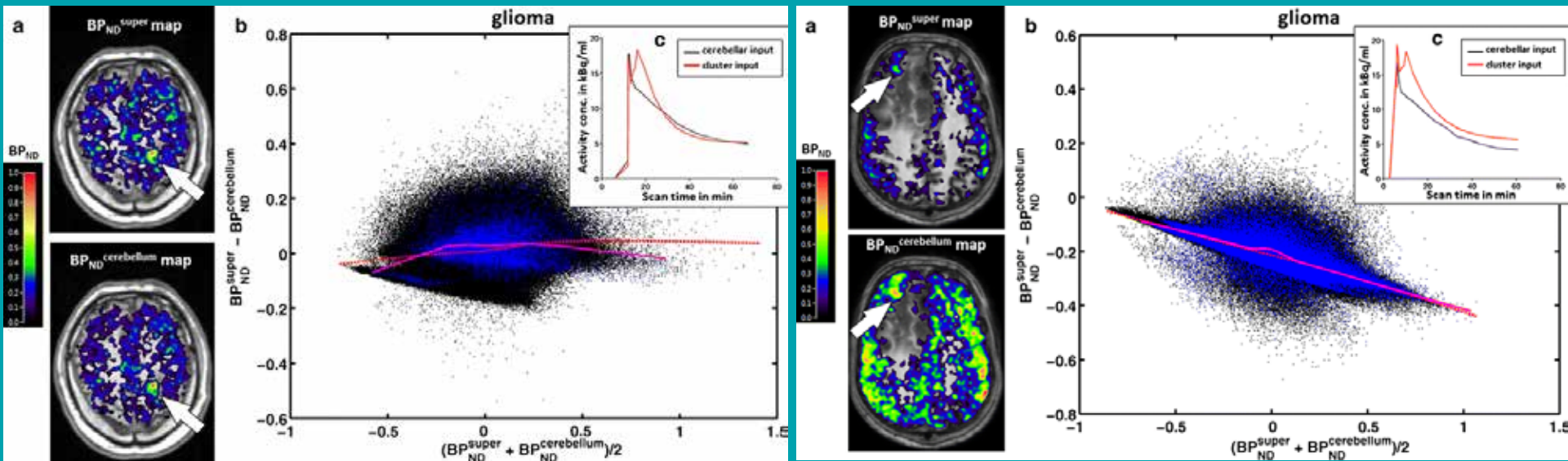


Figure 3. [¹¹C]PK11195 and [¹⁸F]DPA-714 mean uptake values between 20 and 60 min post-injection (expressed as percentage of injected dose per cm³, mean±SD (A) and Core/contralateral ROIs ratio (B)) of the 7 animals scanned with both tracers successively within 24 h (2 animals with no lesion are not shown on these graphs, although their exclusion did not affect the outcome of the statistical analysis). * Significantly different from [¹¹C]PK11195 values, #, significantly different from the contralateral side of the same tracer (Wilcoxon paired test, p<0.05).

[¹¹C]-(*R*)PK11195 tracer kinetics in the brain of glioma patients and a comparison of two referencing approaches

Zhangjie Su • Karl Herholz • Alexander Gerhard •
Federico Roncaroli • Daniel Du Plessis • Alan Jackson •
Federico Turkheimer • Rainer Hinze

Eur J Nucl Med Mol Imaging (2013) 40:1406–1419



Supervised cluster and cerebellar input functions produced consistent BP_{ND} estimates in approximately half of the gliomas investigated, but had a systematic difference in the remainder. **The cerebellar input is preferred.**

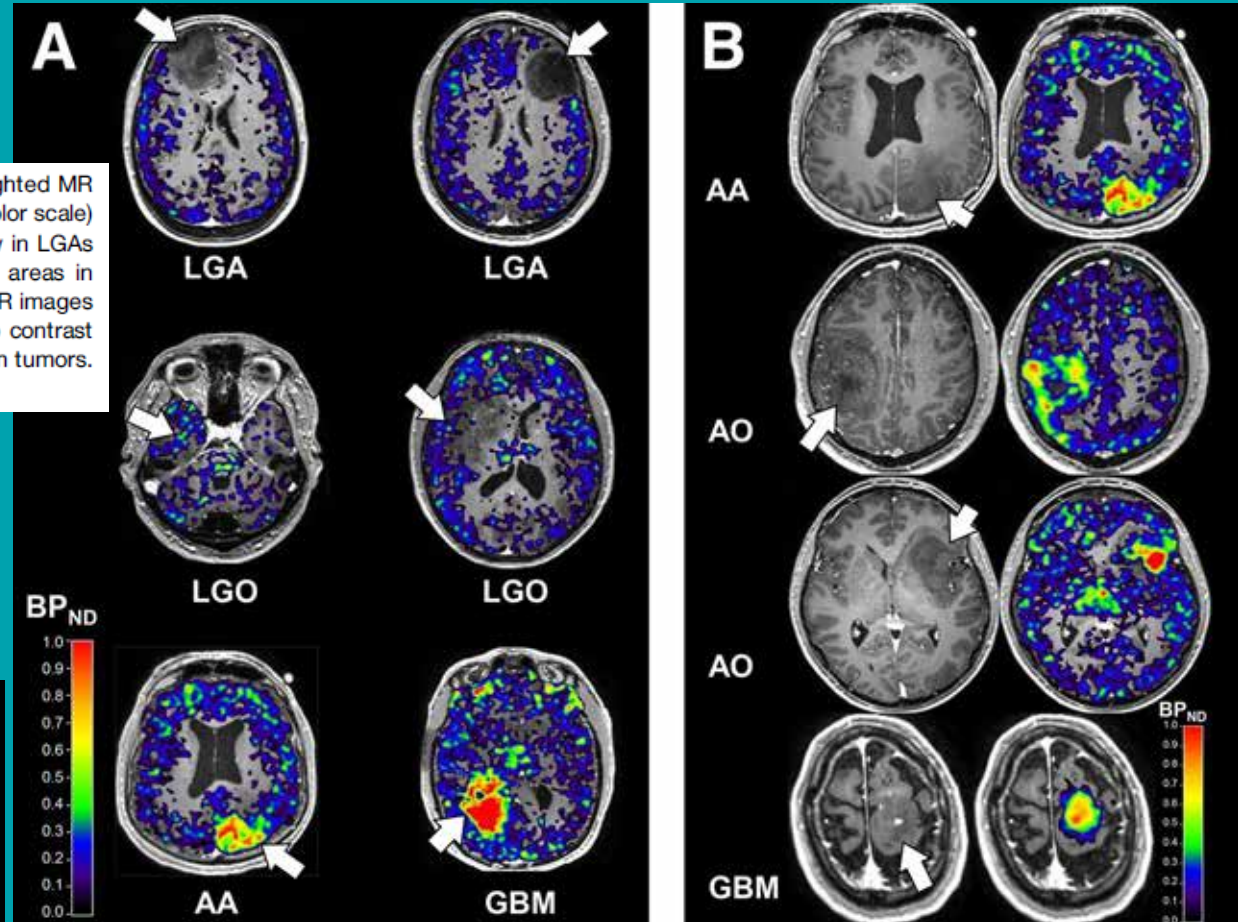
The 18-kDa Mitochondrial Translocator Protein in Human Gliomas: An ^{11}C -(R)PK11195 PET Imaging and Neuropathology Study

J Nucl Med 2015; 56:512–517

JNM The Journal of
NUCLEAR MEDICINE

Zhangjie Su*¹, Federico Roncaroli*², Pascal F. Durrenberger², David J. Coope^{1,3}, Konstantina Karabatsou³, Rainer Hinz¹, Gerard Thompson¹, Federico E. Turkheimer⁴, Karolina Janczar², Daniel Du Plessis⁵, Andrew Brodbelt⁶, Alan Jackson¹, Alexander Gerhard¹, and Karl Herholz¹

FIGURE 2. (A) Coregistered and fused postcontrast T1-weighted MR images (gray scale) and parametric BP_{ND} images (spectrum color scale) of representative cases of LGA, LGO, and HGG; BP_{ND} is low in LGAs whereas high BP_{ND} foci are found in LGOs and high BP_{ND} areas in HGGs (arrows). (B) Coregistered postcontrast T1-weighted MR images and parametric BP_{ND} images in 4 HGGs showing little or no contrast enhancement (arrows) and high ^{11}C -(R)PK11195 binding within tumors. Color bars denote BP_{ND} values.

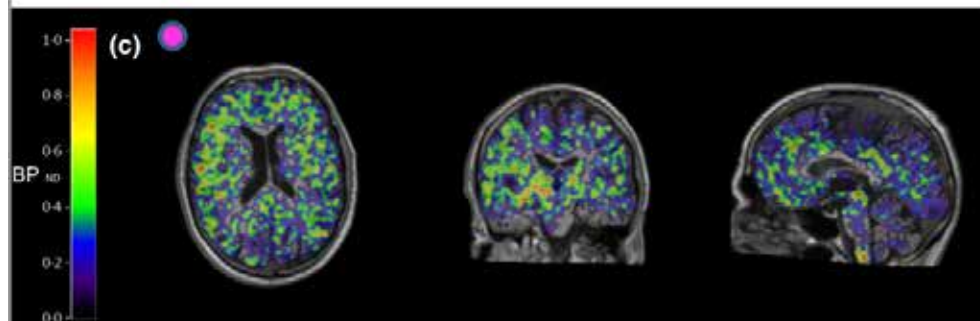
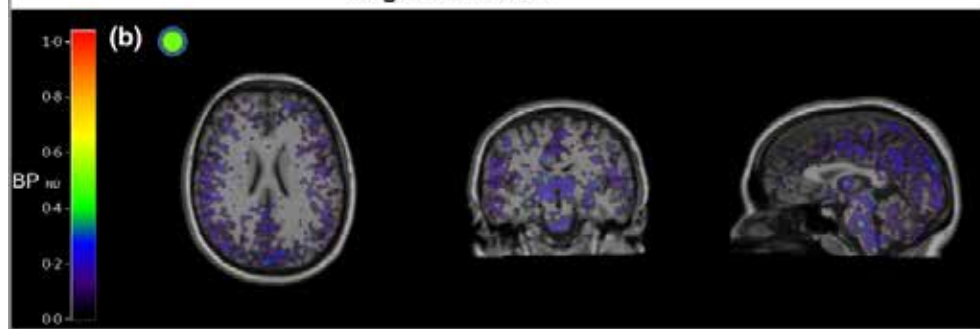
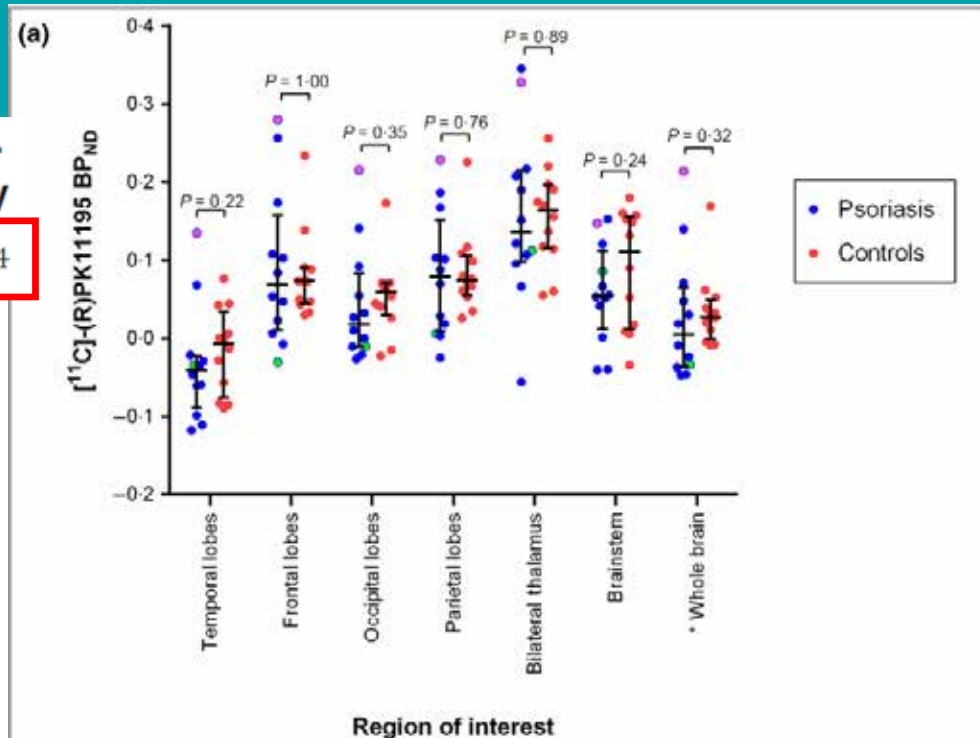


Brain inflammation and psoriasis: a [¹¹C]-(*R*)-PK11195 positron emission tomography study

British Journal of Dermatology (2016) 175, pp1082–1084

H.J.A. HUNTER¹
 R. HINZ²
 A. GERHARD²
 P.S. TALBOT²
 Z. SU²
 G. HOLLAND²
 S.J. HOPKINS³
 C.E.M. GRIFFITHS¹
 C.E. KLEYN¹

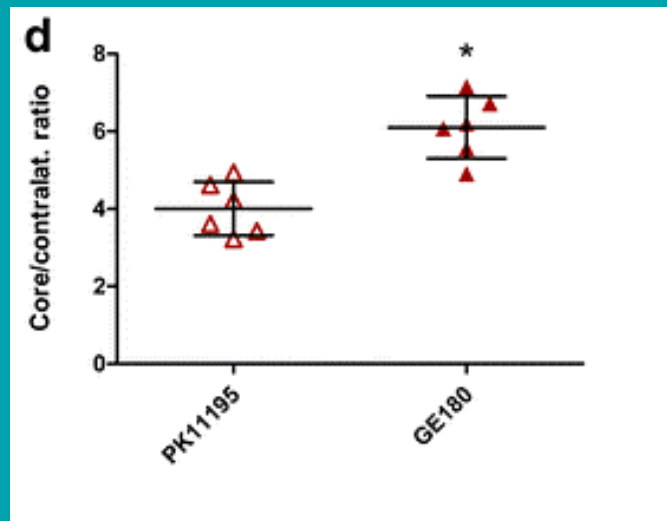
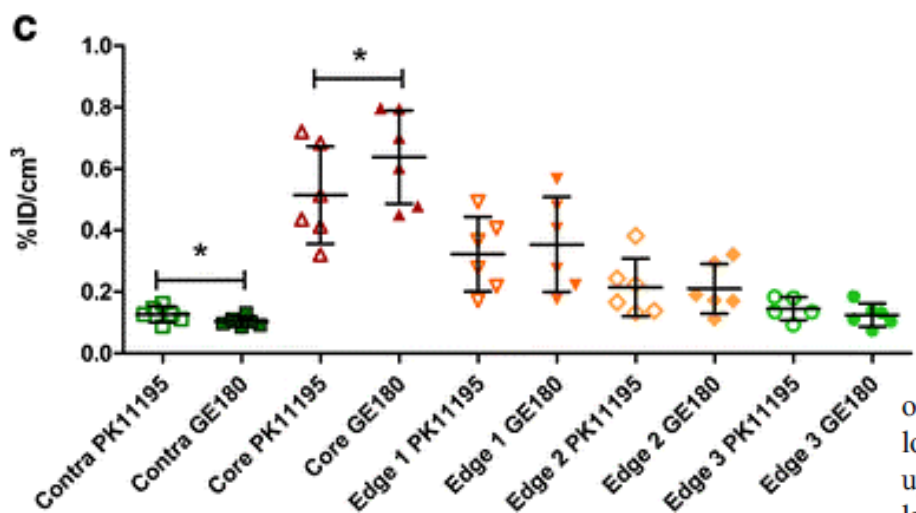
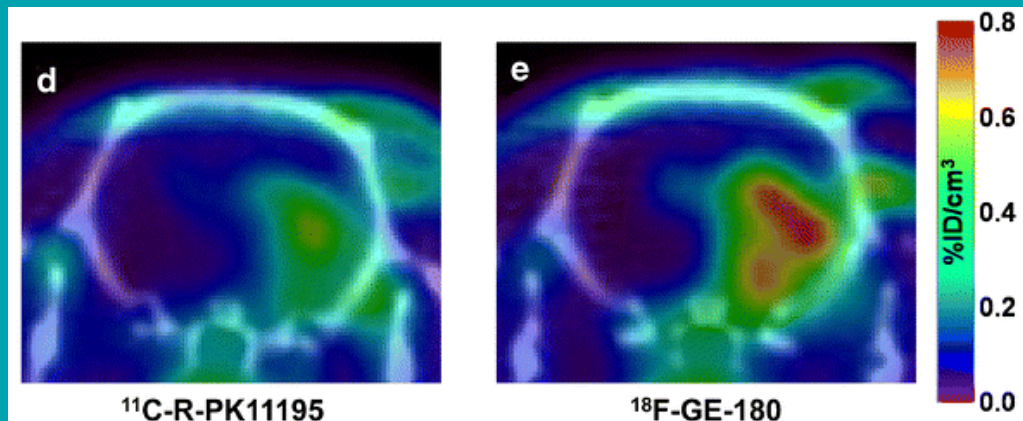
Fig 1. Mean [¹¹C]-(*R*)-PK11195 BP_{ND} across regions of interest (ROIs). (a) There were no significant differences in mean [¹¹C]-(*R*)-PK11195 binding potential (BP_{ND}) across ROIs between groups. Cortical ROIs (bilateral, temporal, frontal, occipital and parietal lobes) were defined using individualized grey matter object maps and subcortical ROIs (bilateral thalamus and brainstem) and whole brain ROIs were defined using individualized unsegmented object maps. Data shown was derived using the cerebellar input function. For each ROI, the median and interquartile ranges are shown. P-values derived from the Mann–Whitney U-test. *Whole brain excluding cerebellum, corpus callosum and brainstem. (b) [¹¹C]-(*R*)-PK11195 BP_{ND} parametric maps superimposed on T1-weighted magnetic resonance imaging scans for a psoriasis patient with low [¹¹C]-(*R*)-PK11195 uptake (transverse, coronal and sagittal planes); represented by green circles on the dot plot. (c) Similar scans for a psoriasis patient with high [¹¹C]-(*R*)-PK11195 uptake; represented by pink circles on the dot plot. Colour bars = [¹¹C]-(*R*)-PK11195 BP_{ND}.



^{18}F -GE-180: a novel TSPO radiotracer compared to ^{11}C -R-PK11195 in a preclinical model of stroke

Eur J Nucl Med Mol Imaging (2015) 42:503–511

Hervé Boutin • Katie Murray • Jesus Pradillo •
 Renaud Maroy • Alison Smigova • Alexander Gerhard •
 Paul A. Jones • William Trigg



c Quantification of uptake

on images summed from 40 to 60 min after injection shows significantly lower uptake in healthy tissue (*dark green*) and a significantly higher uptake in the lesion for ^{18}F -GE-180 (*dark red*). **d** Infarct core to contralateral uptake ratios. * $p < 0.05$ between groups ($n = 6$), paired Wilcoxon test

In vivo imaging of brain microglial activity in antipsychotic-free and medicated schizophrenia: a [¹¹C](*R*)-PK11195 positron emission tomography study

Molecular Psychiatry (2016) 21, 1672–1679

SE Holmes¹, R Hinz², RJ Drake³, CJ Gregory¹, S Conen¹, JC Matthews², JM Anton-Rodriguez², A Gerhard¹ and PS Talbot¹

- 8 antipsychotic-naïve moderate-to-severely symptomatic unmedicated patients,
- 8 patients on risperidone or paliperidone long-acting injections,
- 16 healthy controls,
- parametric maps of BP_{ND} with SRTM and bilateral grey matter cerebellum reference tissue input.

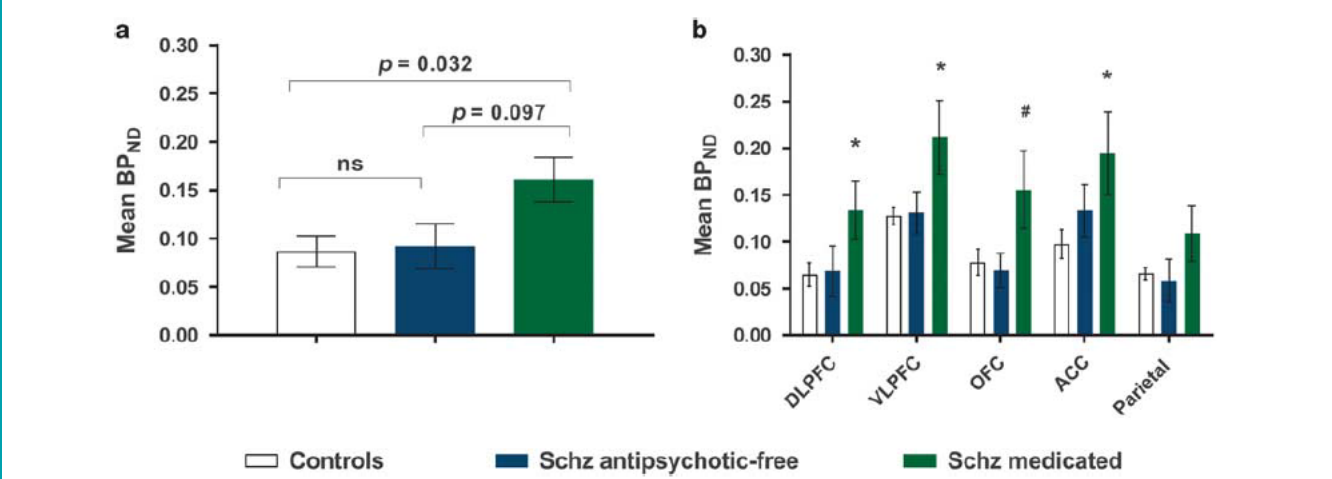


Figure 2. [¹¹C](*R*)-PK11195 binding in antipsychotic-free and medicated patients with schizophrenia compared with healthy controls. (a) Mean cortical BP_{ND} compared between groups, showing statistically significant elevation in medicated patients compared with controls, no difference between antipsychotic-free patients and controls, and trend difference between the two patient groups; (b) BP_{ND} in individual regions of interests (ROIs) compared between groups. *indicates a significant elevation in medicated patients compared with controls at $P < 0.05$; #indicates significant elevation in medicated patients compared with antipsychotic-free patients at $P < 0.05$. ACC, anterior cingulate cortex; BP_{ND}, binding potential; DLPFC, dorsolateral prefrontal cortex; OFC, orbitofrontal cortex; VLPFC, ventrolateral prefrontal cortex.

- Mean cortical BP_{ND} not altered in drug-free patients,
- significantly higher in medicated patients (mean +88%),
- uniform across ROIs (no group * region interaction),
- most significant in DLPFC, VLPFC and ACC.

Comparative Evaluation of Three TSPO PET Radiotracers in a LPS-Induced Model of Mild Neuroinflammation in Rats

Mol Imaging Biol (2017) 19:77–89

Sujata Sridharan,¹ Francois-Xavier Lepelletier,¹ William Trigg,² Samuel Banister,³ Tristan Reekie,³ Michael Kassiou,^{3,4} Alexander Gerhard,¹ Rainer Hinz,¹ Hervé Boutin¹

Fig. 3. Average TACs for cerebellum (*black*) and contralateral (*grey*) reference regions for (R)-[¹¹C]PK11195, [¹⁸F]GE-180 and [¹⁸F]DPA-714 in LPS animals. At 40–60 min, the cerebellar uptake (%ID/cm³) was significantly higher for all three tracers ($p = 0.001$) than the contralateral uptake

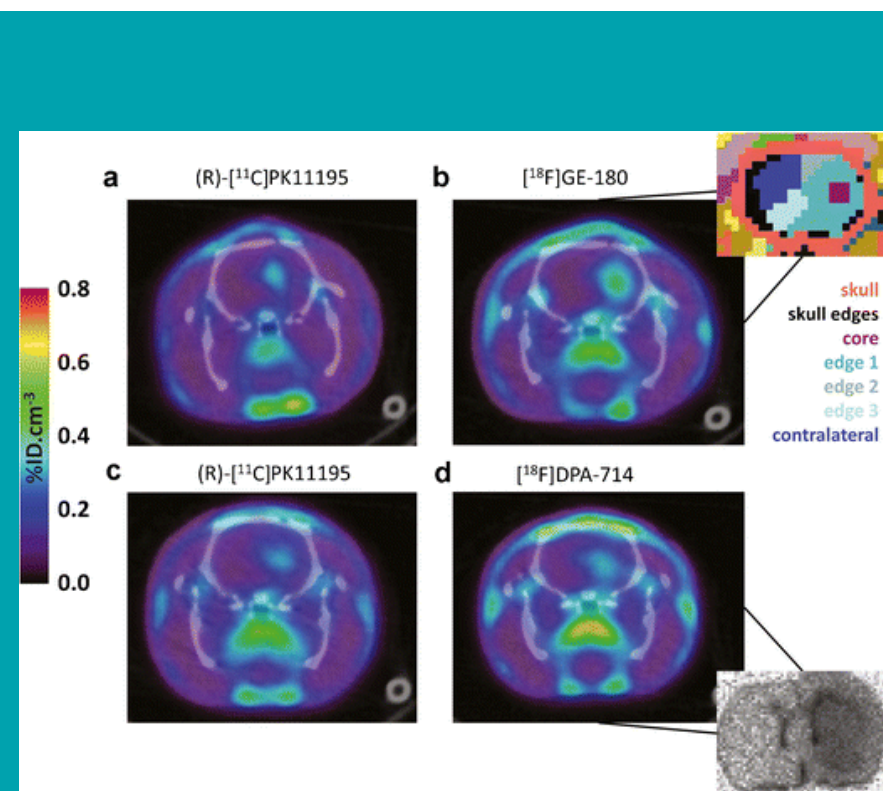
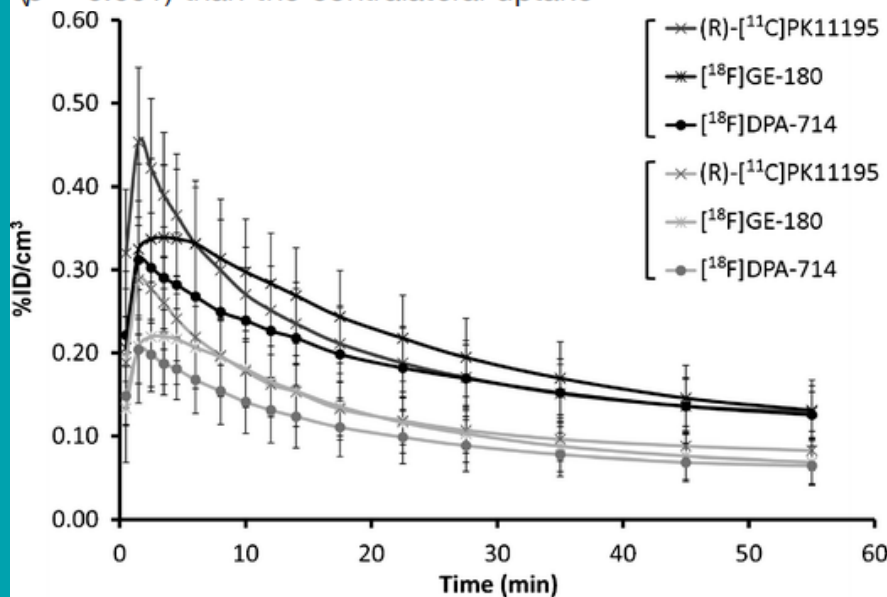


Fig. 4. Co-registered (sum 40–60 min) PET/CT images of representative animals dual-scanned with **a** and **c** (R)-[¹¹C]PK11195 followed by either **b** [¹⁸F]GE-180 (top) or **d** [¹⁸F]DPA-714 (*bottom*). *Inset top*: example of regions defined by automatic segmentation. *Inset bottom*: [¹⁸F]DPA-714 autoradiographic image showing increased specific uptake in the right striatum

Multi-modal imaging of long-term recovery post-stroke by positron emission tomography and matrix-assisted laser desorption/ionisation mass spectrometry

Fiona Henderson^{1,2}  | Philippa J. Hart³ | Jesus M. Pradillo⁴ | Michael Kassiou⁵ | Lidan Christie¹ | Kaye J. Williams² | Herve Boutin¹ | Adam McMahon¹ 

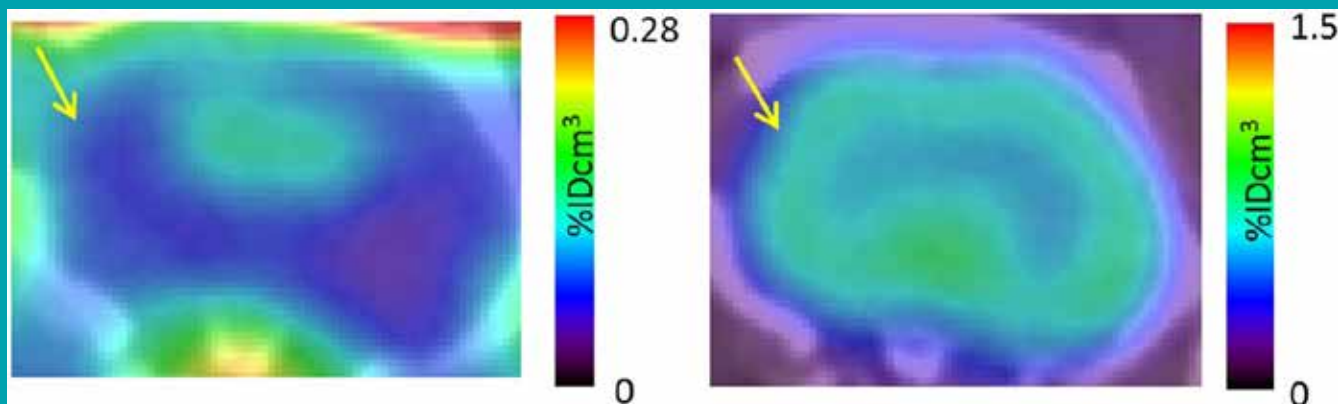


FIGURE 2 . [¹⁸F]-DPA-714 (left) and IAM6067 (right) PET scans of a rat brain 3 months post-ischaemia, showing TSPO and S1R receptors, respectively. Arrows have been drawn to indicate the area of the original infarct [Color figure can be viewed at wileyonlinelibrary.com]

Three months post-stroke, PET detects no substantial neuroinflammation in the peri-infarct area (Figure 2). We have previously shown that [¹⁸F]-DPA-714 can be used as a PET tracer to image TSPO post-ischaemia;³² however, these scans were carried out less than 1 week post-stroke. Neuroinflammation is expected to be at its most aggressive in the first 2 weeks post-stroke,^{33–35} with Martin et al showing a peak of TSPO expression at day 11, using [¹⁸F]-DPA-714 PET. Few imaging

Elevated Translocator Protein in Anterior Cingulate in Major Depression and a Role for Inflammation in Suicidal Thinking: A Positron Emission Tomography Study

Sophie E. Holmes, Rainer Hinz, Silke Conen, Catherine J. Gregory, Julian C. Matthews, Jose M. Anton-Rodriguez, Alexander Gerhard, and Peter S. Talbot

Biological Psychiatry January 1, 2018; 83:61–69

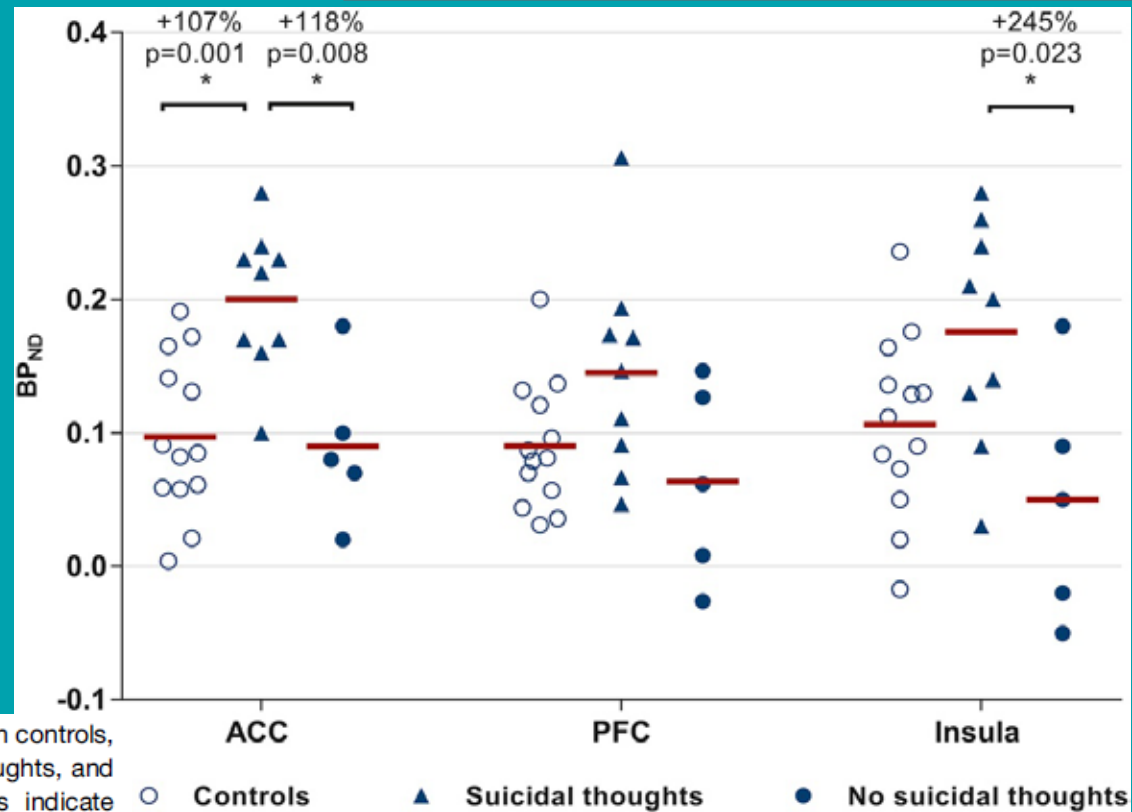


Figure 2. Regional [¹¹C](R)-PK11195 binding potential (BP_{ND}) in controls, patients with major depressive disorder (MDD) with suicidal thoughts, and patients with MDD without suicidal thoughts. Horizontal bars indicate means. Open circles represent control subjects (*n* = 13), closed triangles represent patients with MDD with suicidal thoughts (*n* = 9), and closed circles represent patients with MDD without suicidal thoughts (*n* = 5). Asterisk (*) indicates significant at *p* < .05. ACC, anterior cingulate cortex; PFC, prefrontal cortex.

Assessing Inflammation in Acute Intracerebral Hemorrhage with PK11195 PET and Dynamic Contrast-Enhanced MRI

J Neuroimaging 2018;28:158-161.

Kamran A. Abid*, Oluwaseun A. Sobowale*, Laura M. Parkes, Josephine Naish, Geoff J.M. Parker, Daniel du Plessis, David Brough, Jack Barrington, Stuart M. Allan, Rainer Hinz, Adrian R. Parry-Jones

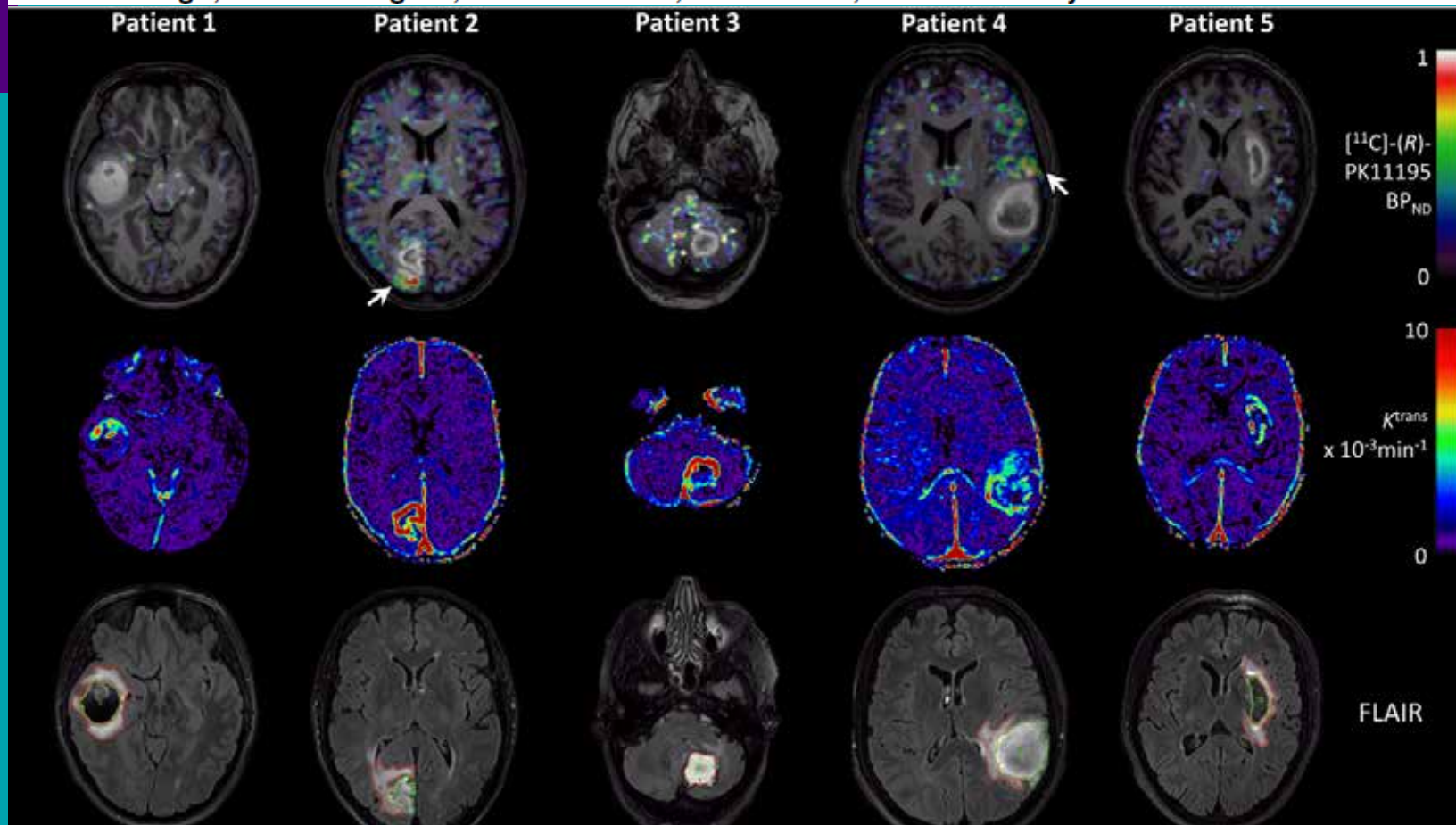


Fig 2. Representative parametric maps of $[^{11}\text{C}]-(R)\text{-PK11195}$ PET binding potential (BP_{ND}) (superimposed on to T_1 -weighted images) and volume transfer constant (K^{trans}) with fluid-attenuated inversion recovery (FLAIR) images from each patient with regions of interest for hematoma (green) and edema (red). Increased $[^{11}\text{C}]-(R)\text{-PK11195}$ binding is indicated in patients 2 and 4 by arrows.

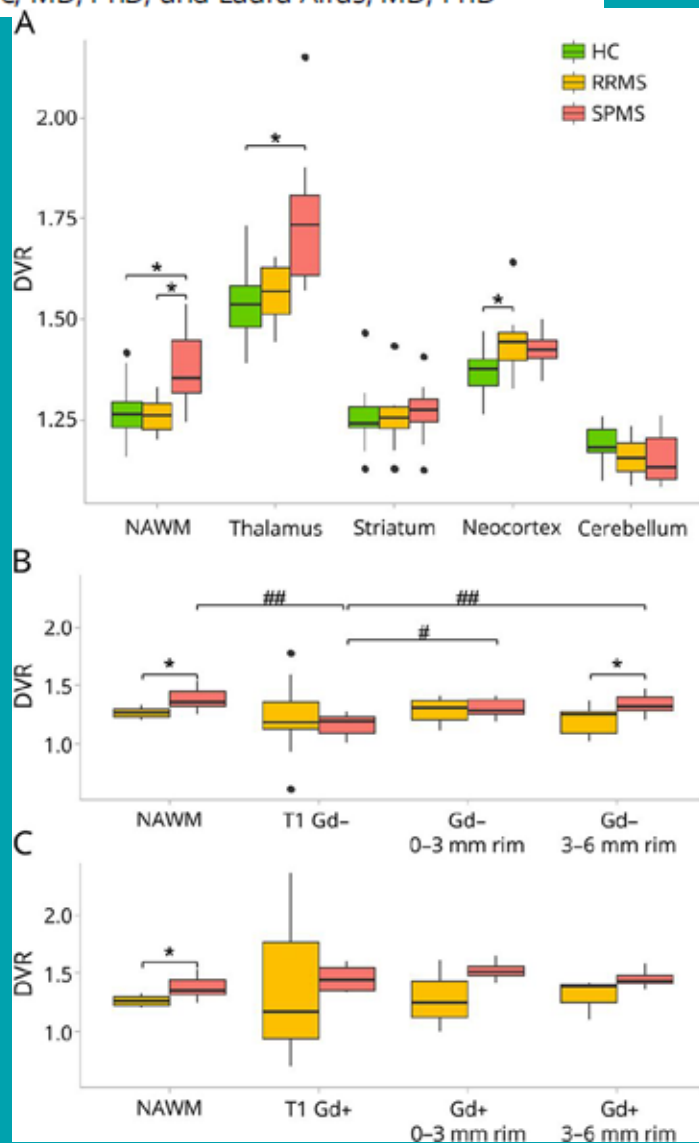
Microglial activation, white matter tract damage, and disability in MS

Neurol Neuroimmunol Neuroinflamm 2018;5:e443.

Eero Rissanen, MD, PhD, Jouni Tuisku, MSc, Tero Vahlberg, MSc, Marcus Sucksdorff, MD, Teemu Paavilainen, MD, PhD, Riitta Parkkola, MD, PhD, Johanna Rokka, PhD, Alexander Gerhard, MD, Rainer Hinz, PhD, Peter S. Talbot, MD, PhD, Juha O. Rinne, MD, PhD, and Laura Airas, MD, PhD

Figure 2 Region of interest (ROI)-specific [¹¹C](R)-PK11195 binding in patients with relapsing-remitting MS (RRMS), patients with secondary progressive MS (SPMS), and controls

Radioligand binding by group among healthy controls (HC, n = 17), patients with RRMS (n = 10), and patients with SPMS (n = 10) in non-lesion-associated ROIs (A), gadolinium-negative lesion-associated ROIs (B), and gadolinium-positive lesion-associated ROIs (C). Each boxplot represents the group median, 1st and 3rd quartiles, minimum and maximum, and outliers (black dots) of distribution volume ratio (DVR) values in each ROI. NAWM = normal-appearing white matter; T1 Gd- = T1-hypointense, gadolinium-negative lesion ROI (including all T1 Gd- lesions); Gd- 0-3 mm rim = perilesional circular ROI 0-3 mm from the edge of gadolinium-negative lesions; Gd- 3-6 mm rim = perilesional circular ROI 3-6 mm from the edge of gadolinium-negative lesions; T1 Gd+ = T1-hypointense, gadolinium-positive lesion ROI (including all T1 Gd+ lesions); Gd+ 0-3 mm rim = perilesional circular ROI 0-3 mm from the edge of gadolinium-positive lesions; Gd+ 3-6 mm rim = perilesional circular ROI 3-6 mm from the edge of gadolinium-positive lesions. *Analysis of age as a covariate, $p < 0.05$. #Repeated-measures analysis of variance (ANOVA), $p < 0.05$. ##Repeated-measures ANOVA, $p < 0.001$.



Inflammation and vascular permeability correlate with growth in sporadic vestibular schwannoma

Daniel Lewis[○], Federico Roncaroli, Erjon Agushi, Dominic Mosses, Ricky Williams, Ka-loh Li, Xiaoping Zhu, Rainer Hinz, [○]Ross Atkinson, Andrea Wadeson, Sharon Hulme, Helen Mayers, Emma Stapleton, Simon K. L. Lloyd, Simon R. Freeman, Scott A. Rutherford, Charlotte Hammerbeck-Ward, D. Gareth Evans, Omar Pathmanaban, Alan Jackson, Andrew T. King, and David J. Coope

Neuro-Oncology

neuroonc/noy177 | Advance Access date 2 November 2018

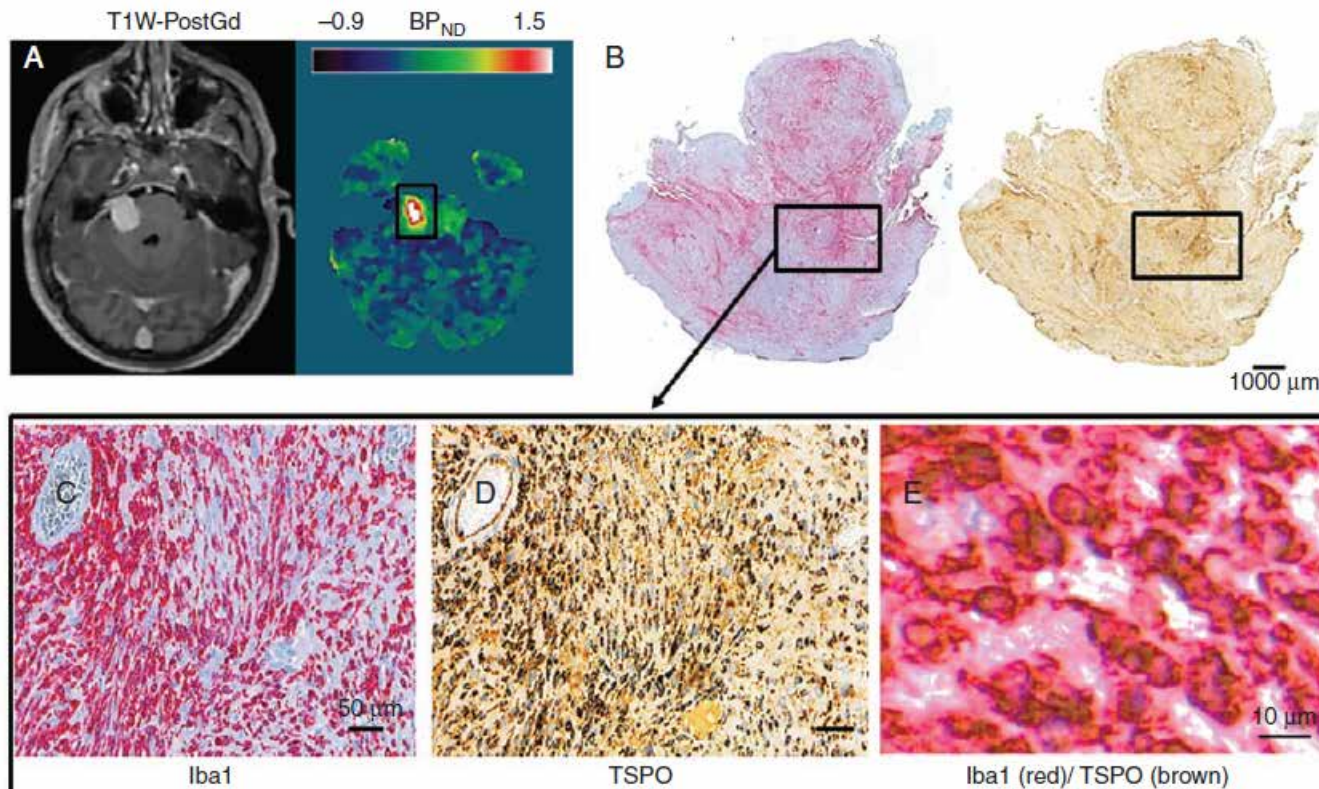
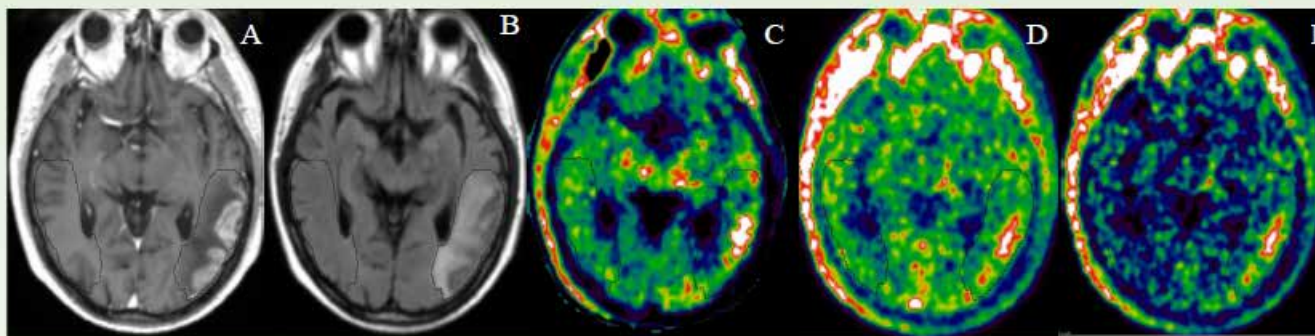


Fig. 4 Spatial colocalization between Iba1 and TSPO in a fast growing VS. Representative axial image sections (*left, T1W post-gadolinium image; right, coregistered parametric map of [11C]-(R)-PK11195 BPND*) from a 25-year-old male (*patient 3*) with a right-sided rapidly growing VS (A). Immunostains (*left, Iba1; right, TSPO*) from the same tumor show the spatial correspondence between Iba1 and TSPO expression (Iba1 red, immunoperoxidase, whole mount; TSPO brown, immunoperoxidase, whole mount) (B). Higher magnification (x20 HPF) demonstrates spatial localization of Iba1 (*left*) and TSPO (*right*) from the area framed in the whole mounts (immunoperoxidase, x20) (C–D). Double immunostained (Iba1/TSPO) proves the colocalization of the 2 signals (immunoperoxidase, x40) (E).

Microglial activation in recent ischemic stroke: comparison of two TSPO tracers



E. Visi¹, R. Hinz¹, W. Trigg², K. McDonald¹, M. Punter³, A. Majid⁴, A. Gerhard¹, K. Herholz¹



(A) MR
Contrast- enhanced
T1- weighted

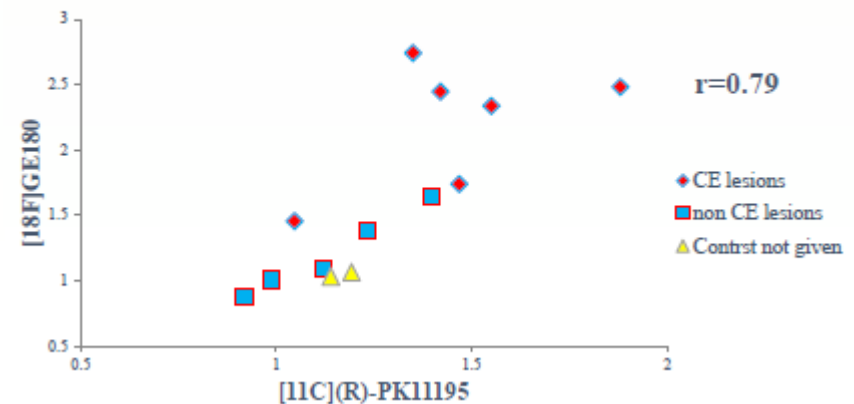
(B) MR FLAIR

(C) [¹¹C](R)-PK11195
PET

(D) [¹⁸F]GE180 PET
- uncorrected

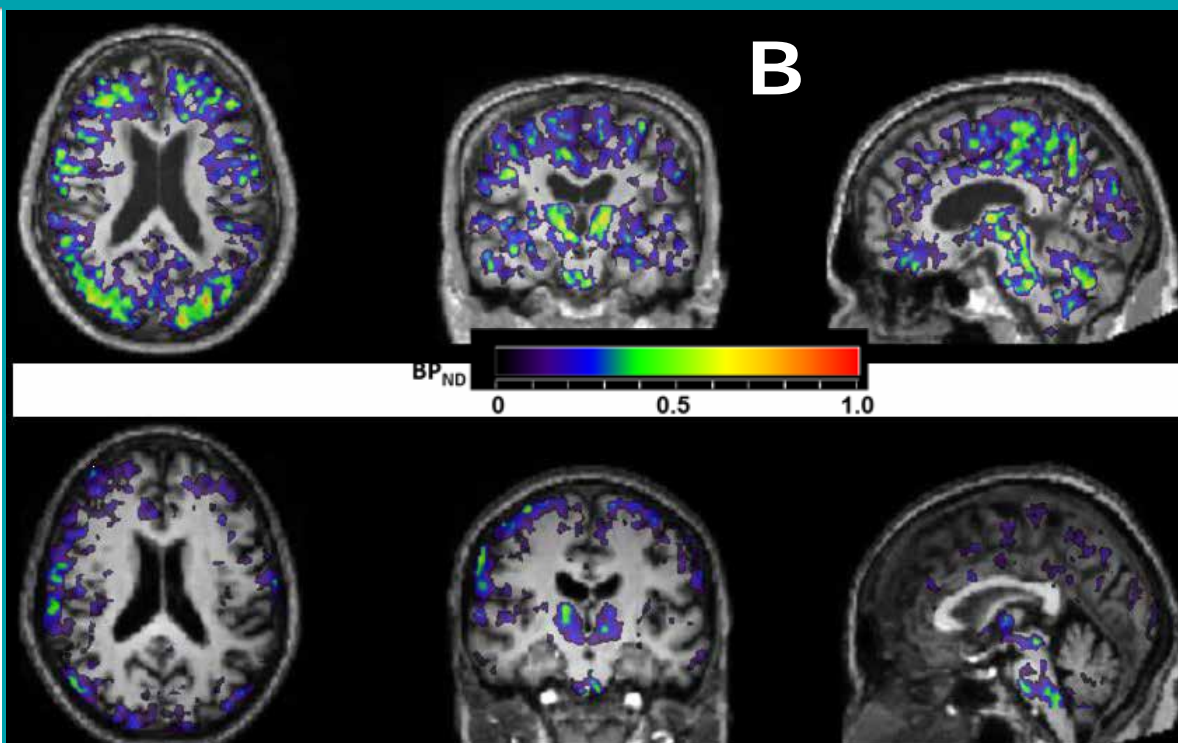
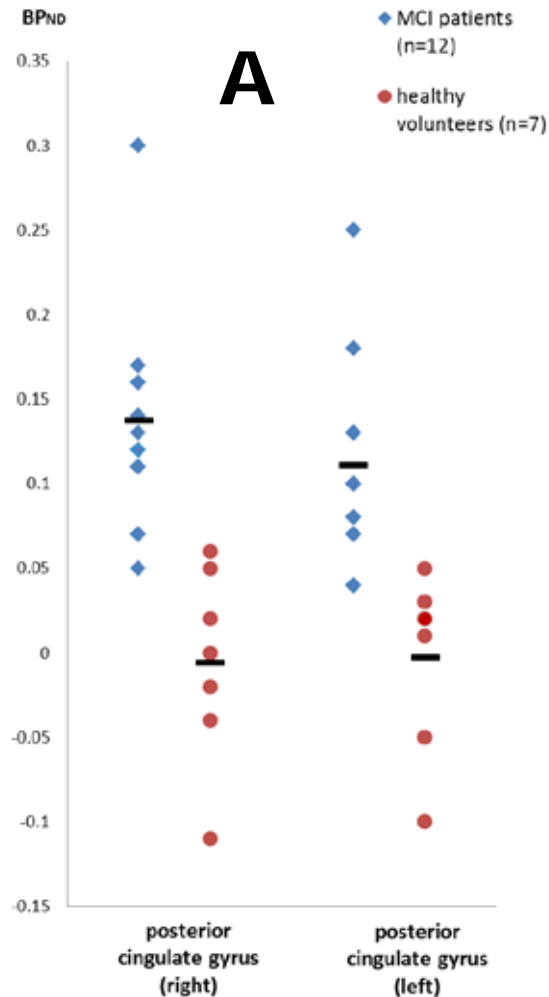
(E) [¹⁸F]GE180 PET
- corrected

Fig.3 TRRs across recent lesions (HAB & MAB) with
correction



Microglial Activation in Patients with Mild Cognitive Impairment: Regional Pattern and the Correlation with Apolipoprotein E Gene Status

Alexander Gerhard, Zhangjie Su, Salman Karim, Jackie Crauther, Matthew Jones, Stephen Hopkins, Rainer Hinz, Nitin Purandare, Alan Jackson, Pippa Tyrrell, Karl Herholz, Alistair Burns



A: Regional mean BP_{ND} in posterior cingulate gyrus of MCI patients compared with controls.

B: Transaxial, coronary and sagittal projections of BP_{ND} parametric images of one MCI patient (upper row) and one healthy volunteer (lower row). The colour bar indicates BP_{ND} values. Images are displayed on each subject's respective T1-weighted MRI scan normalised to the SPM5 T1 brain template.

Neuroinflammation and changes in serotonin metabolism in presymptomatic HD gene carriers: A dual tracer Positron Emission Tomography (PET) study - *First Results.*

Iris Trender-Gerhard & Kathryn R. McDonald, Toby Flanagan, Rainer Hinz, Peter S. Talbot, David Craufurd, Alex Gerhard

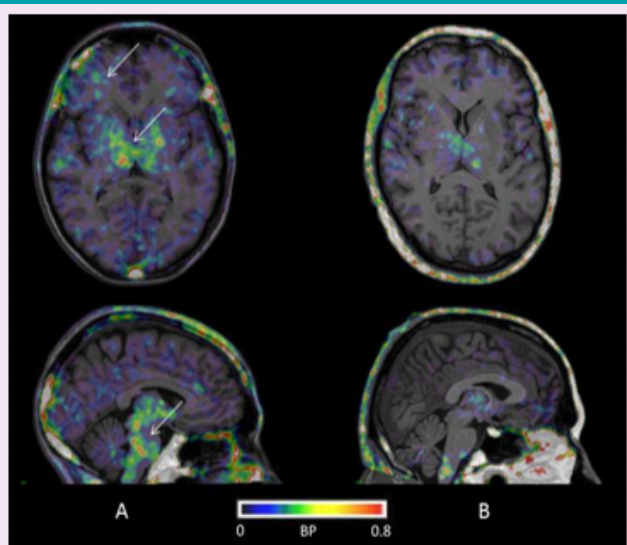


Figure 1: Increased $[^{11}\text{C}](\text{R})\text{-PK11195}$ binding potential (BP) in a presymptomatic HD gene carrier (A) in comparison with a healthy control (B). BP maps are co-registered to the individual T1 MRI. The colour bar denotes BP values 0- 0.8

Increased microglial activation in the preHD participant on the transverse and sagittal sections can be seen in frontal cortical areas, basal ganglia (putamen) and brainstem.

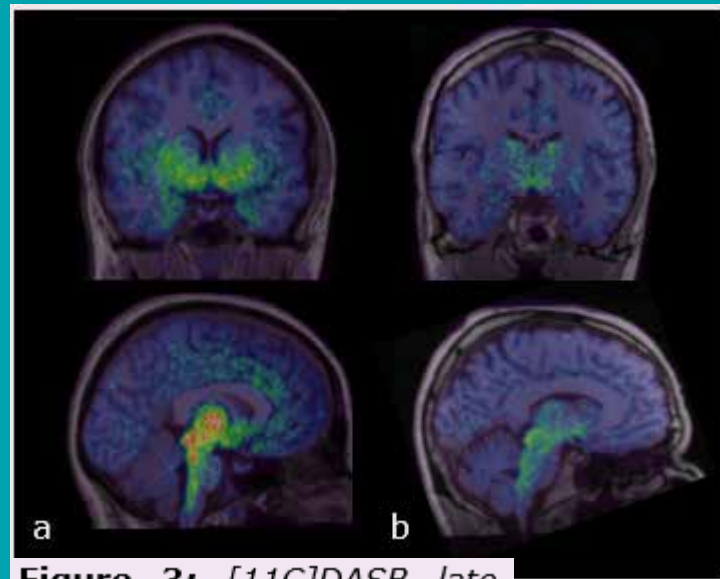


Figure 3: $[^{11}\text{C}]\text{DASB}$ late add images (40-90 minutes), co-registered with the individual MRI of a) a presymptomatic HD gene carrier, b) a healthy control. Coronal and sagittal sections. **DASB binding is increased in brainstem and basal ganglia regions indicating increased serotonin transporter availability.**

Summary and Outlook

Neuroinflammation imaging so far has been a success story in terms of

- prestigious grants attracted to Manchester,
- set of publication outputs, including 3* and 4* for the 2021 REF,
- awarded research degrees (MPhil, MD, PhD),
- national and international collaborations, networking, interdisciplinary approaches to science, contacts with industry (General Electric, Pfizer).

Current developments

- PET/MR utilisation: MRC Confidence in Concept award „*In vivo* characterization of the inflammatory component of carotid plaques using PET/CT and PET/MR in order to develop non-invasive prognostic imaging markers for stroke”,
- ^{18}F labelled GMP tracers required: [^{18}F]GE-180, [^{18}F]DPA-714 -> opportunities for new collaborations, for instance with Sheffield?
- search for neuroinflammation imaging targets post TSPO: imidazoline 2 binding sites ([^{11}C]BU99008), purinergic P2X7 receptor ([^{11}C]JNJ54173717, [^{18}F]JNJ64413739, [^{11}C]SMW139), ... ?

Acknowledgements

PhD students and Research Fellows

- David Coope, Matthew Jones
- Salman Karim, Zhangjie Su
- Kamran Abid, Hamish Hunter
- Glenn Holland, Sophie Holmes
- Sujata Sridharan, Seun Sobowale
- Mark Pinkham, Eszter Visi
- Kathryn McDonald, Tsepoo Goerttler
- Silke Conen, Catherine Gregory
- Erjon Agushi, Daniel Lewis

Colleagues and Collaborators

- Hervé Boutin, Federico Roncaroli
- Federico Turkheimer, Paul Edison, David Brooks (London)
- Ronald Boellaard, Adriaan Lammertsma (Amsterdam)
- Chris Buckley, Will Trigg (GE Healthcare Amersham)
- Jouni Tuisku, Eero Rissanen, Laura Airas (Turku)

Manchester Clinical PIs

- Pippa Tyrrell, Alistair Burns
- Karl Herholz, Alan Jackson
- Alexander and Iris Gerhard
- Adrian Parry-Jones
- Elise Kleyn, Chris Griffiths
- Peter Talbot, Bill Deakin



**Study volunteers and Staff at the
Wolfson Molecular Imaging Centre.**